Impact of alkyl side chains on the photovoltaic and charge mobility properties of naphthodithiophene-benzothiadiazole copolymers

Wang, Bao; Zhang, Ji; Tam, Hoi Lam; Wu, Bo; Zhang, Weifeng; Chan, Miu Shan; Pan, Feng; Yu, Gui; Zhu, Furong; Wong, Man Shing

Published in:
Polymer Chemistry

DOI:
10.1039/c3py00961k

Published: 07/02/2014

Document Version:
Peer reviewed version

Journal Name

Dynamic Article Links ►

Cite this: DOI: 10.1039/c0xx00000x

www.rsc.org/xxxxxx

ARTICLE TYPE

Impact of Alkyl Side Chains on the Photovoltaic and Charge Mobility Properties of Naphthodithiophene-Benzothiadiazole Copolymers

Bao Wang,[a] Ji Zhang,[c] Hoi Lam Tam,[b] Bo Wu,[b] Weifeng Zhang,[c] Miu Shan Chan,[a] Feng Pan,[d] Gui Yu,*[c] Furong Zhu*[b] and Man Shing Wong*[a]

Received (in XXX, XXX) Xth XXXXXXXXX 20XX, Accepted Xth XXXXXXXXX 20XX

DOI: 10.1039/b000000x

A series of 5,6-*bis*(2-ethylhexyloxy)naphtho[2,1-b:3,4-b']dithiophene and 4,7-bis(3-alkylthiophen-2-yl)-2,1,3-benzo[c][1,2,5]thiadiazole alternating copolymers, **PNB-C*n*** with different alkyl chains, varying from 8-carbon (C8, 2-ethylhexyl) to 16-carbon (C16, hexadecyl) chain attached onto thienyl moieties were designed and synthesized. The effect of the conjugated copolymer side chain on the photovoltaic and charge mobility properties of organic solar cells (OSCs) and polymer field-effect transistors (PFETs) was investigated. It is found that the short alkyl side chains on **PNB-C*n*** copolymers are favourable for the efficient operation of bulk heterojunction (BHJ) OSCs, while the long alkyl side chains enhance charge mobility of PFETs. As a result, the BHJ OSCs fabricated from the blend of **PNB-C2,6** and $PC_{71}BM$, using diiodooctane as a solvent additive, yielded a power conversion efficiency of 4.8% and the solution-processed bottom gate bottom contact type PFETs fabricated from **PNB-C16** exhibited a hole mobility of 3.4×10^{-2} cm^2 $V^{-1}s^{-1}$ with a current on/off ratio of 10^6. Our results suggest that copolymers constructed from 5,6-*bis*(2-ethylhexyloxy)naphtho[2,1-b:3,4-b']dithiophene and 4,7-*bis*(3-alkylthiophen-2-yl)-2,1,3-benzo[c][1,2,5]-thiadiazole are very stable, and solution-processable organic semiconductors for application in organic electronics.

Introduction

Bulk heterojunction (BHJ) organic solar cells (OSCs) are currently attracting a great deal of attentions due to the promise of low cost, solution-processability, lightweight, flexibility as well as potential as an alternative renewable energy technology.[1] The BHJ OSCs based on donor-acceptor type molecular/polymer system is one of the most extensively explored approaches for high performance devices as the molecular and functional properties of the organic semiconducting materials such as the optical energy gap, the highest occupied molecular orbital (HOMO) and lowest unoccupied molecular orbital (LUMO) levels as well as the charge mobility can be easily modulated and tuned through chemical structure modification.[2] With the development of new low bandgap donor materials, the effective fabrication processes such as using solvent annealing,[3] thermal annealing[4] and solvent additives[5] to proper control the interpenetrating network morphology of a material blend, as well as the optimized device structure, the power conversion efficiencies (PCE) of the BHJ OSCs based on solution-processable p-type conjugated polymers and n-type fullerene derivatives have recently reached PCE of 8-9% for single junction[6] and 10-11% for tandem OSCs.[7] In general, factors limiting the PCE of the BHJ OSCs are the poor sunlight harvesting efficiency[8] and the low charge carrier transport efficiency[9] of organic semiconductors. Hence, the development of high-performance donor materials is of crucial for further performance improvement of OSCs, which still remains a challenge to the scientific community.

In addition to the choice of the electron-rich and electron-deficient moieties, the lateral substituent(s) that attached onto the donor-acceptor polymer backbone, dependent on the nature, location, length, bulkiness of substituent(s) would exert significant effect on the optical, electronic properties and morphology of the polymer thin-film.[10] Thus, this can provide an alternative tool or means to tune the functional properties of polymer in the solid state. Furthermore, the proper solubilizing lateral substituent(s) can improve the solubility and processability of the highly π-conjugated and high molecular-weight donor-acceptor polymers.[10a]

Recently, much effort has been devoted on understanding the influence of side chains on the functional and optoelectronic properties of conjugated polymers. You and coworkers[10b] have demonstrated that the length and shape of the alkyl side chain attached onto the main chain of naphtha[2,1-b:3,4-b]dithiophene-4,7-di(thiophen-2-yl)benzothiadiazole (PNDT-DTB) copolymer could strongly influence not only the optical absorption and the morphology of the thin films, but also the open-circuit voltage (V_{oc}) and short circuit current density (J_{sc}) of the resulting BHJ OSCs. Studies of poly(3-alkylthiophene) (P3AT) showed that the nature, size, and length of the alkyl side chains could be used to enhance the molecular properties and photovoltaic device performance of the corresponding BHJ OSCs.[11] It was recently shown that long alkyl side chains in P3AT could assist the self-

assembly of the ordered film via alkyl chain interactions; on the other hand, sufficient long alkyl chain could act as an insulating barrier hindering the charge transport.[12] The influence of side chains was also found in other donor-acceptor polymeric systems in which the material properties, the charge mobility and the photovoltaic device performances varied strongly with variable side chains.[6a, 13]

We have previously shown that 5,6-*bis*(2-ethylhexyloxy)naphtho[2,1-b:3,4-b']dithiophene and 4,7-*bis*(3-decylthiophen-2-yl)-2,1,3-benzo[c][1,2,5]thiadiazole alternating low bandgap copolymer exhibited a broad absorption range and promising device performance in BHJ OSCs.[14] To further investigate and optimize the alkyl side chains on various functional, charge mobility and photovoltaic properties of this copolymer system, a series of 5,6-*bis*(2-ethylhexyloxy)naphtho[2,1-b:3,4-b']dithiophene and 4,7-*bis*(3-alkylthiophen-2-yl)-2,1,3-benzo[c][1,2,5]thiadiazole alternating copolymers, **PNB-C*n*** with different alkyl side chains, varying from 8-carbon (C8, 2-ethylhexyl) to 16-carbon (C16, hexadecyl) chain attached onto 3-position of thienyl moieties were designed and synthesized. Fig. 1 shows the molecular structures of the copolymers, **PNB-C*n***, where *n* = 2,6; 10; 12; 14 and 16.

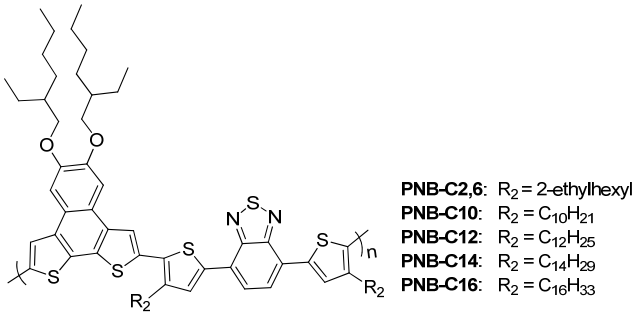

Fig.1 5,6-*Bis*(2-ethylhexyloxy)naphthodithiophene and 4,7-*bis*(3-alkylthiophen-2-yl)-2,1,3-benzothiadiazole alternating copolymers, **PNB-C*n*** with different alkyl side chains.

The synthetic routes for the key electron-rich intermediate, 5,6-*bis*(2-ethylhexyloxy)-2,9-*bis*(*tri*-*n*-butylstannyl)naphthodithiophene, **5** and electron-deficient moieties, 4,7-*bis*(3-alkylthiophen-2-yl)-2,1,3-benzothiadiazole, **11a-e** are outlined in **Scheme 1**.

Compound 1-7,[14] 8a - 11a,[13a] 8b - 11b,[10b] and 8c,d,e - 11c,d,e[15] were synthesized according to the reported procedures with optimized conditions. The detailed procedures are given in electronic supplementary information (ESI). The alternating copolymers, **PNB-C*n*** were synthesized by the Stille polycondensation reaction of 5,6-*bis*(2-ethylhexyloxy)-2,9-*bis*(*tri*-*n*-butylstannyl)naphthadithiophene, **5** with 4,7-bis(5-bromo-3-alkylthiophen-2-yl)-2,1,3-benzo-thiadiazole, **11a-e** using $Pd(PPh_3)_4$ as catalyst in DMF at 120 °C for 48 h under N_2 (**Scheme 1**). All the copolymers showed good solubility in chloroform, THF and chlorobenzene.

Experimental section

Materials Synthesis

All the reagents were used as purchased unless otherwise mentioned.

Synthesis of PNB-C2,6. To a 50 mL round-bottom flask containing 3-(2-ethylhexyl)thiophene (69 mg, 0.10 mmol), 5,6-*bis*(2-ethylhexyloxy)-2,5-*bis*(tri-*n*-butylstannyl)naphtha[2,1-b:3,4-b']-dithiophene (108 mg, 0.10 mmol) were added $Pd(PPh_3)_4$ (10 mg). After three successive deoxygenation-refilling with N_2 cycles, DMF (30 mL) were added via a syringe. The polymerization was carried out at 120 ^oC for 48 h under N_2. The polymer was precipitated in MeOH and collected by filtration. Low-molecular-weight oligomers were removed by Soxhlet extraction with MeOH, hexane and DCM, respectively. The remaining high molecular-weight solid was extracted with chloroform. The desired polymer was precipitated from methanol, collected and dried in vacuum for 12 h affording the product as a black solid (60 mg, 59%), M_n = 72 kDa, PDI = 2.1.

Results and Discussion

Physical and thermal stability properties

The number average molecular weight (M_n) of copolymers, determined by gel permeation chromatograph (GPC) using polystyrene as standard and THF as eluent, were in the range of 44−47 KDa for **PNB-C*n***, where n = 10, 12, 14, and 16 and 72 KDa for **PNB-C2,6** with a polydispersity index (PDI) of 1.6-2.1. All the copolymers showed high thermal stability with onset decomposition temperatures with 5% weight loss (T_d) in the range of 353−389 °C as determined by thermal gravimetric analysis (TGA) (Table 1). There was no glass transition state observed for all the copolymers as revealed by differential scanning calorimetry (DSC) analysis. The physical and thermal stability data of the copolymers are summarized in Table 1.

Table 1 Molecular weight and thermal properties of copolymers

Polymer	M_n [a] (kDa)	M_w [a] (kDa)	PDI[a]	T_d[b](°C)
PNB-C2,6	72	151	2.1	389
PNB-C10	45	86	1.9	368
PNB-C12	47	85	1.8	385
PNB-C14	44	70	1.6	353
PNB-C16	47	85	1.8	373

[a] Molecular weights determined by gel permeation chromatography (GPC) in THF using polystyrene as standard. [b] Onset decomposition temperature (5% weight loss) measured by TGA.

Optical and electrochemical properties

The absorption spectra of copolymers measured in THF and thin film are shown in Fig. 2. Both spectra of copolymers exhibit two major absorption bands, in which the weak absorption is at around 430 nm corresponding to π-π* transitions, while the strong and broad absorption is around 610 nm corresponding to intramolecular charge transfer (ICT) between the donor and acceptor moieties.[16] Increasing the size of alkyl substituent attached on the two thienyl rings, from 2-ethylhexyl to hexadecyl group, does not alter the absorption characteristics in THF because of the good solubility of all copolymers with identical π-conjugated backbone.[10b] There is a slight red shift in the absorption spectra in thin films (Fig. 2b) as compared to those in solution which is attributed to the improved π-π stacking in solid state films. In addition, there is a small variation of absorption cut-off in thin films within the series. As revealed from the optimized geometries of these polymers obtained by the DFT

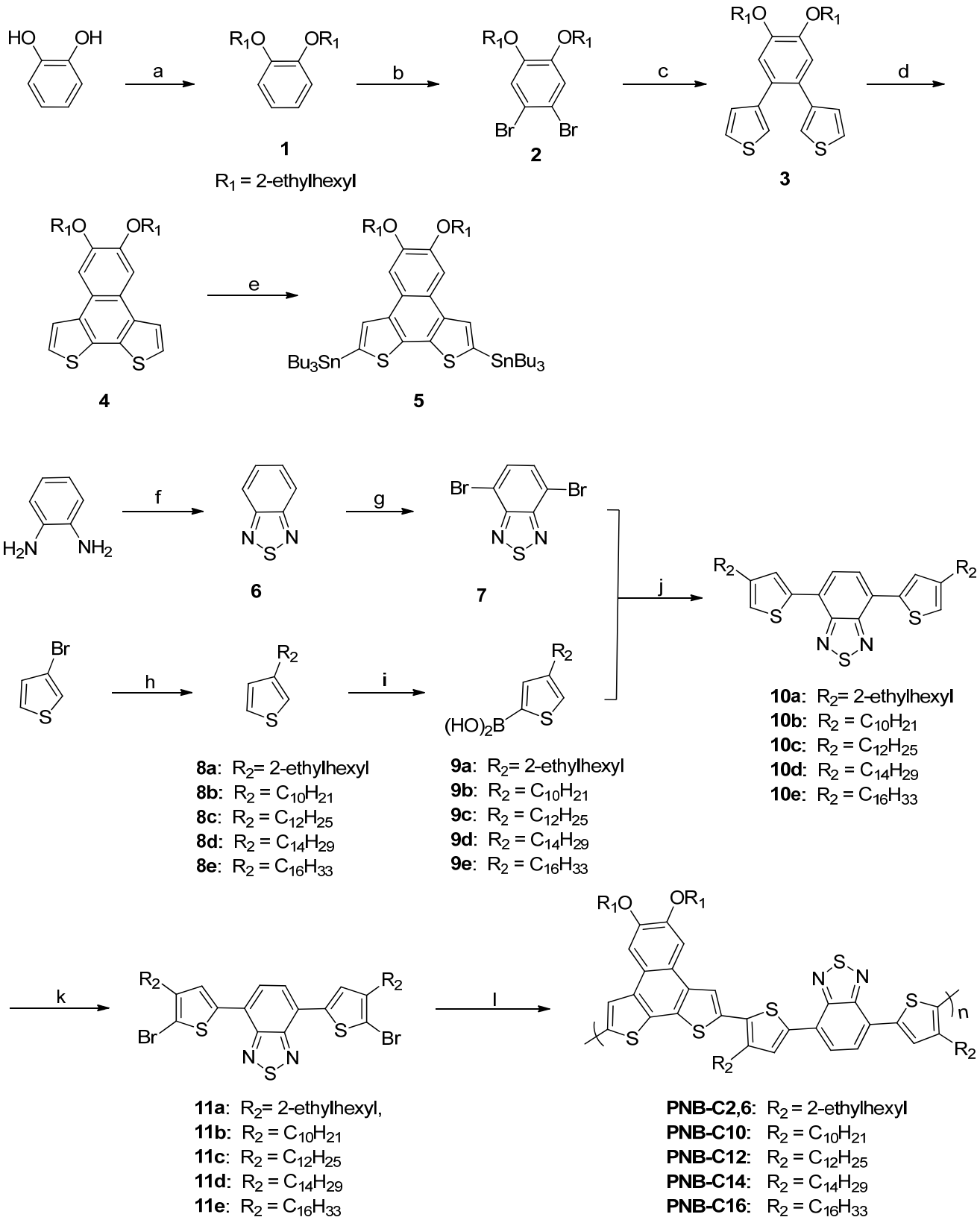

Scheme 1 Synthesis of co-polymers **PNB-C*n***. Reagents and conditions: a) DMSO, KOH, 2-ethylhexyl bromide, 88%; b) NBS, $CHCl_3$/AcOH, 86%; c) 3-thiopheneboronic acid, $Pd(PPh_3)_4$, 2M K_2CO_3, THF, 84%; d) $FeCl_3$, $MeNO_2$, DCM, 78%; e) *n*-BuLi, Bu_3SnCl, 94%; f) $SOCl_2$, Et_3N, DCM, 76%; g) Br_2, HBr, 91%; h) (i) Mg, R_2Br, (ii) $Ni(dppp)Cl_2$, 77−90%; i) *n*-BuLi, $B(OMe)_3$, 70 − 80%; j) $Pd(PPh_3)_4$, 2M K_2CO_3, THF, reflux overnight, 75% - 87%; k) NBS, $CHCl_3$/AcOH, 86 − 90%; l) **5**, DMF, $Pd(PPh_3)_4$, 120 ºC, 48 h.

calculations at the B3LYP 6-31G(d) level, the dihedral angles between the napthodithiophene and thienyl units of polymers **PNB-C10** and **PNB-C2,6** are very similar (Fig. 3). Thus, such a small variation is not likely due to the difference in conformation of the polymer backbone. The absorption edges of these copolymer films reach ~750 nm which corresponds to an optical bandgap of ~1.68 eV.

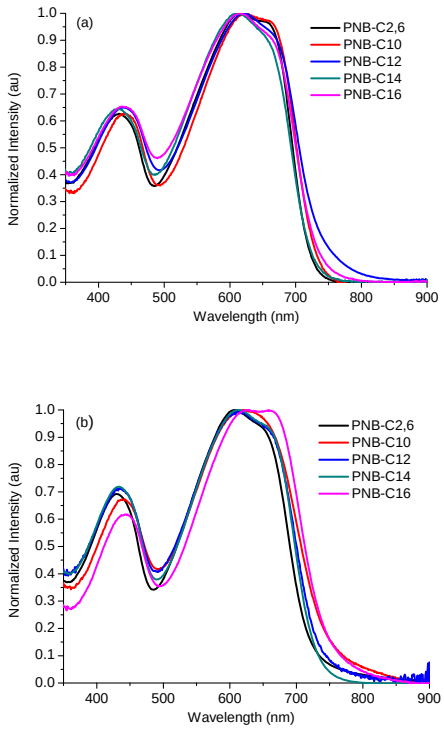

Fig.2 UV-Vis absorption spectra of copolymers in (a) THF and (b) thin films.

To investigate the redox potentials of these copolymers, cyclic voltammetry measurements were performed in dry CH_3CN (with 0.1 M $(n\text{-Bu})_4NPF_6$) using $Ag/AgNO_3$ as a reference electrode. The **PNB-C*n*** copolymers show very similar redox behaviour with one irreversible oxidation couple with onset oxidation potentials (E_{onset}^{ox}) in the range of 0.41 − 0.51 V and one irreversible reduction wave with onset reduction potentials (E_{onset}^{red}) in the range of -1.23 − -1.33 V. The HOMO energy levels of copolymers were determined by calculating from the onset oxidation potentials with ferrocene as an external standard.

The LUMO energy level was determined from the measured HOMO energy level and the optical bandgap energy (see Table 2). The HOMO energy levels of these copolymers are estimated to be around -5.20 eV and the LUMO energy levels are estimated to be around at -3.51 eV. The results indicate that these copolymers are fairly stable in air, an important characteristic of organic semiconductors, which is a prerequisite for the application in PFETs and OSCs.

Photovoltaic properties

BHJ OSCs were fabricated using **PNB-C*n*** copolymers as the electron donor and [6,6]-phenyl-C_{71}-butyric acid methyl ester

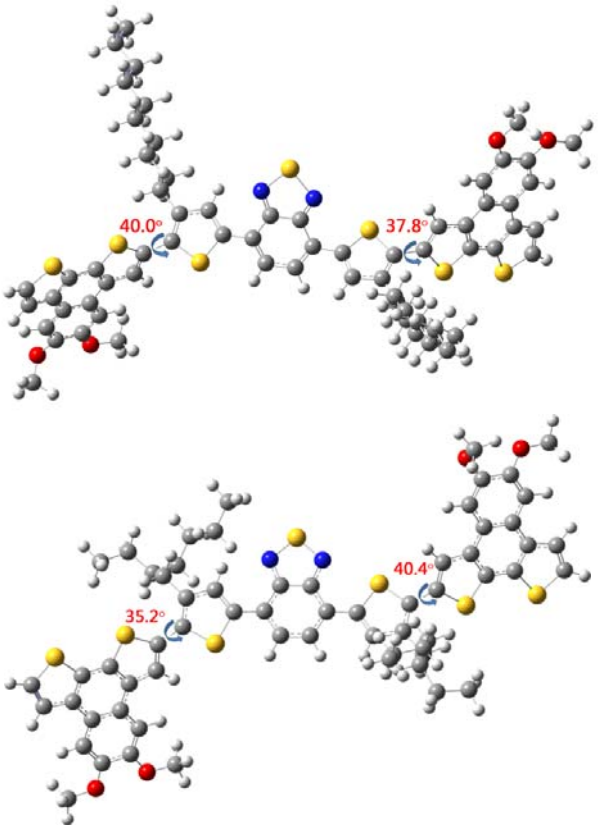

Fig. 3 DFT-optimized geometries of the monomeric unit of polymer **PNB-C10** and **PNB-C2,6** with alkoxy chains replaced with methoxy chains to simplify the calculations

Table 2 Optical and electrochemical data of copolymers

Polymer	E_g^{opt} (eV)[a]	E_{onset}^{ox} (V)[b]	E_{onset}^{red} (V)[b]	HOMO (eV)[b]	LUMO (eV)[c]
PNB-C2,6	1.72	0.46	-1.26	-5.19	-3.47
PNB-C10	1.64	0.41	-1.23	-5.14	-3.50
PNB-C12	1.69	0.43	-1.32	-5.16	-3.47
PNB-C14	1.70	0.47	-1.28	-5.20	-3.50
PNB-C16	1.66	0.51	-1.33	-5.26	-3.60

[a] Calculated from the intersection of the tangent on the low energy edge of the absorption spectrum with the baseline. [b] Determined by CV. HOMO = - (4.73 + E_{onset}^{ox}) eV. [c] LUMO = (HOMO + E_g^{opt}) eV.

($PC_{71}BM$) as the electron acceptor with a conventional device structure of ITO/PEDOT:PSS (30 nm)/polymer:$PC_{71}BM$ (100 nm) (1:2)/Al (100 nm) and an active cell area of 9 mm^2. The device performance measured under AM 1.5 simulated solar illumination at an irradiation intensity of 100 mW cm^{-2}, is greatly affected by the fabrication parameters such as the use of solvent additives and with or without thermal annealing process. The performance of BHJ OSCs fabricated under different process conditions including the weight ratio of polymer to $PC_{71}BM$ in the blend layer, the volume ratio of 1,8-diiodooctane (DIO) additive in the solvent, the effect of post-annealing was investigated (see ESI). It is interesting to find that increasing the ratio of DIO from 0%, 1% to 3% v/v, the fill factor (FF) and J_{sc} of devices fabricated from the copolymer:$PC_{71}BM$ blends progressively increase.[5b, 5d] Meanwhile, the post-deposition

thermal annealing show a dramatic effect on the device performance with which the FF, J_{sc} and V_{oc} of the devices can be further enhanced (ESI).[3b, 17] The optimum device performance was obtained using 6 mg/mL of polymer in chlorobenzene containing 3 vol% DIO for spin-coating with a copolymer:$PC_{71}BM$ ratio of 1:2 (w/w) with film thickness of 100 nm after post-annealing at 80 °C for 10 min. The *J-V* characteristics and the incident photon to current efficiency (IPCE) of the optimized OSCs are shown in Fig. 4.

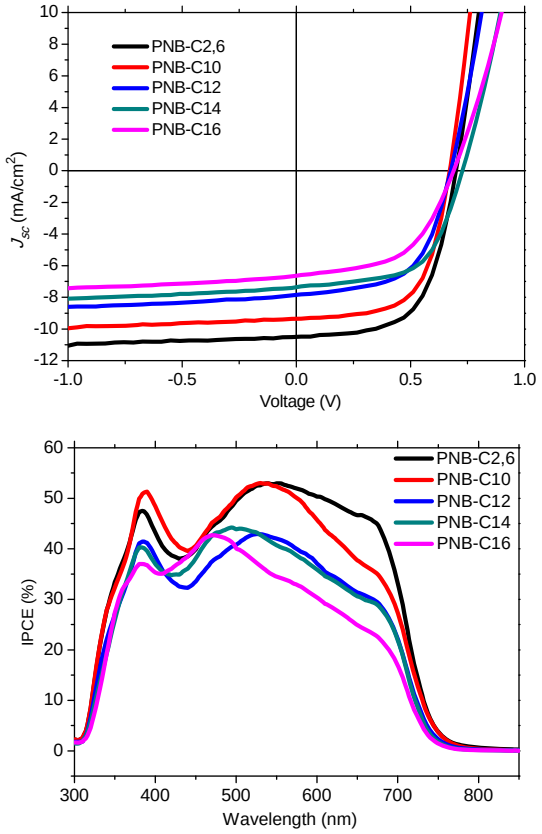

Fig. 4 The photocurrent density–voltage (*J-V*) characteristics (left) and IPCE spectra (right) of optimized OSCs

A summary of the photovoltaic properties of **PNB-C*n***–based OSCs fabricated using 3% DIO solvent additive with post-annealing at 80 °C is shown in Table 3. It is clearly shown that OSCs fabricated from **PNB-C*n*** copolymers have a high FF of 0.58 − 0.63, suggesting that π-conjugated backbone of **PNB-C*n*** with different alkyl side chains have good charge-transport properties.[18] They also exhibit a similar V_{oc} in the range of 0.67 − 0.73 V, which is in good agreement with the measured HOMO energy levels. Nevertheless, there is a dramatic difference in the J_{sc} among these BHJ OSCs leading to a variation in PCE. There is an increasing tendency of J_{sc} and PCE of the OSCs as the alkyl side chain gets smaller in size. As a result, **PNB-C2,6**, with the shortest branched side chains afforded the best device performance with a V_{oc} of 0.70 V, a J_{sc} of 11.13 mA cm^{-2} and a FF of 0.61, giving rising to a PCE of 4.8%. Although these co-polymers exhibit almost identical absorption behaviour, the IPCE curves consistently show that the **PNB-C2,6** based device exhibits a broad and strong photoresponse with the highest efficient photoconversion efficiency than the other homologous in the spectral range between 300 and 750 nm.

Table 3 Summary of the photovoltaic characteristics of devices with ITO/PEDOT:PSS/**PNB-C*n***:$PC_{71}BM$/Al configuration using 3% DIO as a solvent additive with post annealing at 80 °C.

Polymer	J_{sc}/mA cm^{-2}	V_{oc}/V	FF (%)	PCE (%)
PNB-C2,6	10.5 (11.13)[a]	0.70	61	4.5 (4.8)[a]
PNB-C10	9.36 (9.92)[a]	0.68	63	3.93 (4.2)[a]
PNB-C12	7.85 (8.32)[a]	0.68	58	3.3 (3.5)[a]
PNB-C14	7.35 (7.79)[a]	0.73	59	3.2 (3.4)[a]
PNB-C16	6.64 (7.04)[a]	0.67	63	2.8 (3.0)[a]

[a] IPCE calibrated value.

The film morphologies of **PNB-C*n***:$PC_{71}BM$ blends with and without DIO additive of **PNB-C2,6** and **PNB-C16** were investigated using atomic force microscopy (AFM) as shown in Fig. 5. The isolated and large domains seen in the AFM height images are formed from both of the blend films fabricated from chlorobenzene without using solvent additive. These domains are far larger than typical exciton diffusions lengths (~10 nm),[19] and thus hinder efficient exciton dissociation resulting in low current density. On the contrary, blend films with different DIO solvent additive ratios from 1% to 3%, the films afforded significantly more homogeneous morphologies in which the nanoscale phase separation and bicontinuous interpenetrating networks provide more efficient charge separation and transport. Thus, the

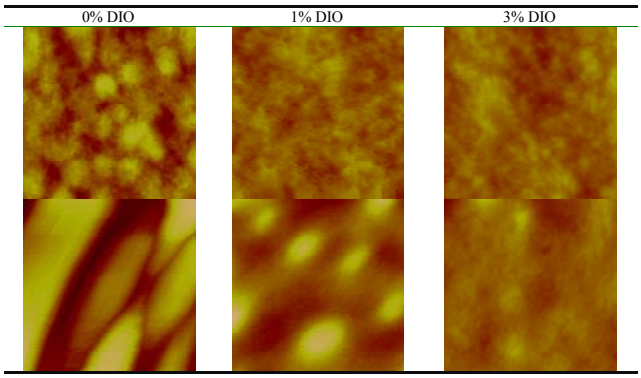

Fig. 5 AFM height images of **PNB-C*n***:$PC_{71}BM$ blend films with different ratio of DIO at a resolution of 1 µm × 1 µm. (top row: **PNB-C2,6** and bottom row: **PNB-C16**).

favourable phase separation results in an enhancement in J_{sc} for **PNB-C2,6** and **PNB-C16** based OSCs from 6.45 mA cm^{-2} to 10.5 mA cm^{-2} and 2.37 mA cm^{-2} to 6.64 mA cm^{-2}, respectively, which is consistent to the recently reported efficient OSCs.

Field-Effect Transistor Mobility

To investigate the charge transport properties of **PNB-C*n*** thin films, bottom-gate bottom-contact configuration (BGBC) PFETs with Au drain and source contacts were fabricated. The active layer was spin-casted onto the octadecyltrichlorosilane (OTS)-modified SiO_2/Si substrates at 1500 rpm for 60 s from a chlorobenzene solution with a concentration of 10 mg/mL using constant channel width of 1400 µm. The performance of PFETs was optimized with channel length and thermal annealing process. A summary of the characteristics of **PNB-C*n***–based PFETs is shown in Table 4. All the transistors based on these copolymers exhibit typical p-type PFET characteristics. Fig. 6

Table 4 Summary of the annealing effect on the performance of **PNB-C*n*** based PFETs treated at different post-annealing temperatures.

Polymer	Annealing T (°C)	μ^a (cm^2 V^{-1} s^{-1})	$I_{on}/I_{off}{}^b$	V_{th}(V)^c
PNB-C2,6	240	0.029	$10^{5\text{-}6}$	1
PNB-C10	240	0.015	10^3	7
PNB-C12	240	0.023	$10^{2\text{-}3}$	6
PNB-C14	240	0.026	$10^{6\text{-}7}$	-14
PNB-C16	200	0.034	10^6	-10

[a] Maximum value of the hole mobility, [b] I_{on}/I_{off} refers to the corresponding on-off ratio, [c] refers to the threshold voltage.

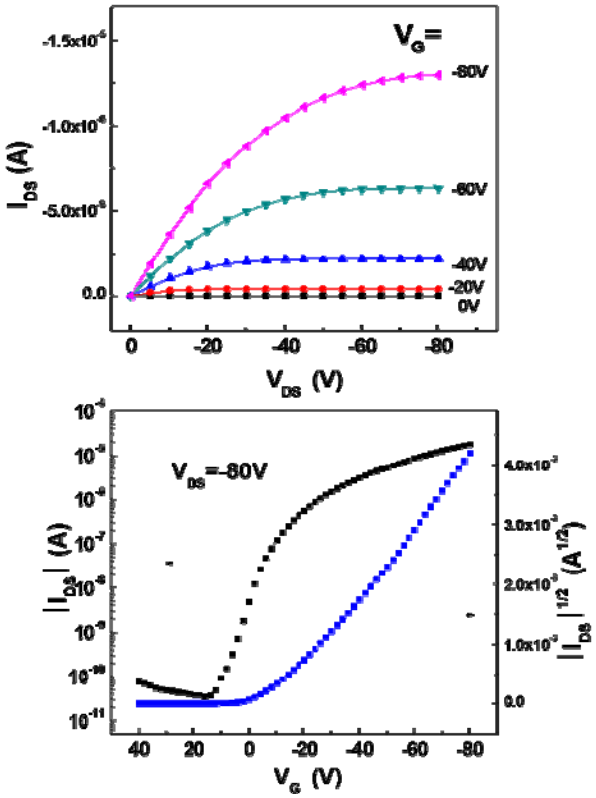

Fig. 6 Typical p-type (up) output and (down) transfer characteristics of **PNB-C16**-based PFETs with a channel length of 48 μm and annealed at 200 °C.

shows typical output and transfer characteristics of the PFETs made with **PNB-C16**. For as fabricated PFETs with a channel length of 8 μm, these copolymers exhibit a hole mobility in the range of $1.8 \times 10^{-3} - 5.0 \times 10^{-3}$ cm^2 V^{-1} s^{-1}. Upon increasing the annealing temperature of these polymeric thin films, there is an obvious enhancement in the hole mobility reaching up to $1.5 \times 10^{-2} - 3.4 \times 10^{-2}$ cm^2 V^{-1} s^{-1} with a current on/off ratio up to 10^6 at the annealing temperature of 200 °C to 240 °C. The increase in the hole mobility of the PFETs upon thermal annealing suggests that the crystallinity of the polymer films and ordered lamellar structure of π-π close packing for polymer backbone are significantly improved at higher annealing temperatures. The results reveal that there is a noticeable increase in the hole mobility for those co-polymers with a similar molecular weight when the linear length of alkyl side chains increases from decyl (C10) to hexadecyl (C16) groups (Table 4 and Fig. 7). The high molecular weight of **PNB-C2,6** can also afford the high hole mobility of 2.9×10^{-2} cm^2 V^{-1} s^{-1} with a current on/off ratio of 10^5.

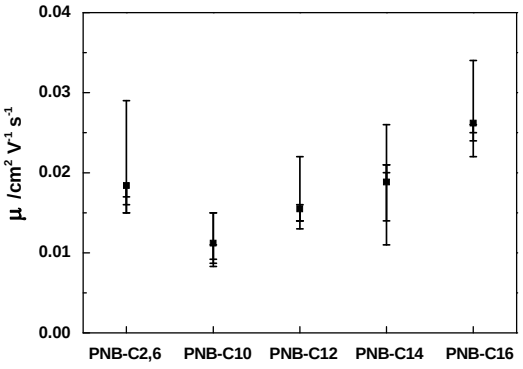

Fig. 7 Statistical plots of the PFETs performance of **PNB-C*n*** based transistors treated at the optimized post-annealing temperatures.

AFM images of polymer thin films were investigated at various annealing temperatures (see ESI). Pristine films showed discontinued surface structure; on the other hand, with film annealing treatment, a fibril-like, well-ordered and bi-continuous morphology was formed, which favours the charge carrier transport and leads to an increase in the hole mobility.

Conclusions

A series of 5,6-*bis*(2-ethylhexyloxy)naphtho[2,1-b:3,4-b']dithiophene and 4,7-*bis*(3-alkylthiophen-2-yl)-2,1,3-benzo[c][1,2,5]thiadiazole alternating copolymers, **PNB-C*n*** with different alkyl side chains attached onto thienyl groups were designed, synthesized and characterized. These copolymers exhibit strong and broad absorption spectra, high thermal stability and appropriate energy levels as p-type materials for organic electronics. The resulting BHJ OSCs fabricated from these copolymers with different alkyl side chains exhibited similar V_{oc} (0.67 - 0.73 V) and FF (0.58 - 0.63) but dramatic difference in J_{sc} values giving rise to the significant variation of device performance. Our results reveal that the shorter the alkyl side chains of the thienyl groups, the higher the J_{sc}, leading to a V_{oc} of 0.70 V, a J_{sc} of 11.13 mA cm^{-2}, a FF of 0.61 and a PCE of 4.8% measured for OSCs fabricated using a blend of **PNB-C2,6** and $PC_{71}BM$. In contrast, the hole mobility is enhanced with an increase in length of the linear alkyl side chains. The solution-processed PFETs fabricated from these copolymers exhibited a high hole mobility up to 0.034 cm^2 V^{-1} s^{-1} with a current on/off ratio of 10^6. Our results demonstrated that **PNB** based-polymer is a promising candidate for further exploration in various high-performance organic electronic devices.

Acknowledgements

The Institute of Molecular Functional Materials and this work are supported by a grant from the University Grants Committee, Areas of Excellence Scheme (AoE/P-03/08) and this work is supported by a grant from the Research Grants Council (Project No. [T23-713/11]) and a grant form the National Science

Foundation of China (51228301).

Notes and references

[a] *Institute of Molecular Functional Materials#, Department of Chemistry and Institute of Advanced Materials, Hong Kong Baptist University, Kowloon Tong, Hong Kong SAR, China. E-mail: mswong@hkbu.edu.hk*
[b] *Department of Physics and Institute of Advanced Materials, Hong Kong Baptist University, Kowloon Tong, Hong Kong SAR, China. E-mail: frzhu@ hkbu.edu.hk*
[c] *Beijing National Laboratory for Molecular Sciences, Institute of Chemistry, Chinese Academy of Sciences, Beijing 100190, P. R. China. E-mail: yugui@iccas.ac.cn*
[d] *School of Advanced Materials, Peking University Shenzhen Graduate School, Shenzhen University Town, Xili, Nanshan District, Shenzhen, 518055, P.R. China*
[#] *Areas of Excellence Scheme, University Grants Committee (Hong Kong)*
† Electronic Supplementary Information (ESI) available: [Materials Characterization, Device Fabrication and Measurements]. See DOI: 10.1039/b000000x/

1 *(a)* M. Helgesen, R. Sondergaard, F. C. Krebs, *J. Mater. Chem*., 2010, **20**, 36; *(b)* S. H. Park, A. Roy, S. Beaupre, S. Cho, N. Coates, J. S. Moon, D. Moses, M. Leclerc, K. Lee, A. J. Heeger, *Nat. Photon*., 2009, **3**, 297; *(c)* H.-Y. Chen, J. Hou, S. Zhang, Y. Liang, G. Yang, Y. Yang, L. Yu, Y. Wu, G. Li, *Nat. Photon*., 2009, **3**, 649; *(d)* J. H. Seo, A. Gutacker, Y. Sun, H. Wu, F. Huang, Y. Cao, U. Scherf, A. J. Heeger, G. C. Bazan, *J. Am. Chem. Soc*., 2011, **133**, 8416.

2 *(a)* J. Roncali, *Macromol. Rapid. Commun*., 2007, **28**, 1761; *(b)* H. Zhou, L. Yang, W. You, *Macromolecules*, 2012, **45**, 607; *(c)* J. Mei, Y. Diao, A. L. Appleton, L. Fang, Z. Bao, *J. Am. Chem. Soc*., 2013, **135**, 6724.

3 *(a)* H. Chen, S. Hu, H. Zang, B. Hu, M. Dadmun, *Adv. Funct. Mater*., 2013, **23**, 1701; *(b)* G. Li, Y. Yao, H. Yang, V. Shrotriya, G. Yang, Y. Yang, *Adv. Funct. Mater*., 2007, **17**, 1636; *(c)* B. Qu, D. Tian, Z. Cong, W. Wang, Z. An, C. Gao, Z. Gao, H. Yang, L. Zhang, L. Xiao, Z. Chen, Q. Gong, *J. Phys. Chem. C*, 2013, **117**, 3272.

4 W. Ma, C. Yang, X. Gong, K. Lee, A. J. Heeger, *Adv. Funct. Mater*., 2005, **15**, 1617.

5 *(a)* J. Peet, J. Y. Kim, N. E. Coates, W. L. Ma, D. Moses, A. J. Heeger, G. C. Bazan, *Nat. Mater*., 2007, **6**, 497; *(b)* S. J. Lou, J. M. Szarko, T. Xu, L. Yu, T. J. Marks, L. X. Chen, *J. Am. Chem. Soc*., 2011, **133**, 20661; *(c)* J. S. Moon, C. J. Takacs, S. Cho, R. C. Coffin, H. Kim, G. C. Bazan, A. J. Heeger, *Nano. Lett*., 2010, **10**, 4005; *(d)* J. K. Lee, W. L. Ma, C. J. Brabec, J. Yuen, J. S. Moon, J. Y. Kim, K. Lee, G. C. Bazan, A. J. Heeger, *J. Am. Chem. Soc*., 2008, **130**, 3619.

6 *(a)* I. Osaka, T. Kakara, N. Takemura, T. Koganezawa, K. Takimiya, *J. Am. Chem. Soc*., 2013, **135**, 8834; *(b)* T. Yang, M. Wang, C. Duan, X. Hu, L. Huang, J. Peng, F. Huang, X. Gong, *Energy Environ. Sci*., 2012, **5**, 8208; *(c)* H.-C. Chen, Y.-H. Chen, C.-C. Liu, Y.-C. Chien, S.-W. Chou, P.-T. Chou, *Chem. Mater*., 2012, **24**, 4766; *(d)* H. Choi, J.-P. Lee, S.-J. Ko, J.-W. Jung, H. Park, S. Yoo, O. Park, J.-R. Jeong, S. Park, J. Y. Kim, *Nano. Lett*., 2013, **13**, 2204; *(e)* C. Cabanetos, A. El Labban, J. A. Bartelt, J. D. Douglas, W. R. Mateker, J. M. J. Fréchet, M. D. McGehee, P. M. Beaujuge, *J. Am. Chem. Soc*., 2013, **135**, 4656; *(f)* Z. He, C. Zhong, S. Su, M. Xu, H. Wu, Y. Cao, *Nat. Photon*., 2012, **6**, 591.

7 *(a)* J. You, L. Dou, K. Yoshimura, T. Kato, K. Ohya, T. Moriarty, K. Emery, C.-C. Chen, J. Gao, G. Li, Y. Yang, *Nat. Commun*., 2013, **4**, 1446; *(b)* J. You, C.-C. Chen, Z. Hong, K. Yoshimura, K. Ohya, R. Xu, S. Ye, J. Gao, G. Li, Y. Yang, *Adv. Mater*., 2013, DOI: 10.1002/adma.201300964.

8 J.-S. Huang, T. Goh, X. Li, M. Y. Sfeir, E. A. Bielinski, S. Tomasulo, M. L. Lee, N. Hazari, A. D. Taylor, *Nat. Photon*., 2013, **7**, 479.

9 *(a)* G. Li, V. Shrotriya, J. Huang, Y. Yao, T. Moriarty, K. Emery, Y. Yang, *Nat. Mater*., 2005, **4**, 864; *(b)* A. Pivrikas, N. S. Sariciftci, G. Juška, R. Österbacka, *Prog. Photovolt: Res. Appl*., 2007, **15**, 677.

10 *(a)* Z. Li, Y. Zhang, S.-W. Tsang, X. Du, J. Zhou, Y. Tao, J. Ding, *J. Phys. Chem. C*, 2011, **115**, 18002; *(b)* L. Yang, H. Zhou, W. You, *J. Phys. Chem. C*, 2010, **114**, 16793.

11 *(a)* P.-T. Wu, G. Ren, S. A. Jenekhe, *Macromolecules*, 2010, **43**, 3306; *(b)* J. Hou, T. L. Chen, S. Zhang, L. Huo, S. Sista, Y. Yang, *Macromolecules*, 2009, **42**, 9217; *(c)* A. Gadisa, W. D. Oosterbaan, K. Vandewal, J.-C. Bolsée, S. Bertho, J. D'Haen, L. Lutsen, D. Vanderzande, J. V. Manca, *Adv. Funct. Mater*., 2009, **19**, 3300; *(d)* Y. D. Park, D. H. Kim, Y. Jang, J. H. Cho, M. Hwang, H. S. Lee, J. A. Lim, K. Cho, *Org. Electron*., 2006, **7**, 514.

12 H. S. Lee, J. H. Cho, K. Cho, Y. D. Park, T *J. Phys. Chem. C*, 2013, **117**, 11764.

13 *(a)* L. Biniek, S. Fall, C. L. Chochos, D. V. Anokhin, D. A. Ivanov, N. Leclerc, P. Lévêque, T. Heiser, *Macromolecules*, 2010, **43**, 9779; *(b)* J. M. Szarko, J. Guo, Y. Liang, B. Lee, B. S. Rolczynski, J. Strzalka, T. Xu, S. Loser, T. J. Marks, L. Yu, L. X. Chen, *Adv. Mater*., 2010, **22**, 5468; *(c)* Q. Peng, X. Liu, D. Su, G. Fu, J. Xu, L. Dai, *Adv. Mater*., 2011, **23**, 4554; *(d)* T. Lei, J.-Y. Wang, J. Pei, *Chem. Mater*., 2013, DIO: 10.1021/cm4018776; *(e)* D. H. Kim, A. L. Ayzner, A. L. Appleton, K. Schmidt, J. Mei, M. F. Toney, Z. Bao, *Chem. Mater*., 2013, **25**, 431; (f) T. Lei, J.-Y. Wang, J. Pei, *Adv. Mater*., 2012. **24**, 6457.

14 B. Wang, S.-W. Tsang, W. Zhang, Y. Tao, M. S. Wong, *Chem. Commun*., 2011, **47**, 9471.

15 S. P. Mishre, A. K. Palai, R. Srivastava, M. N. Kamalasanan, M. Patri, *J. Poly. Sci. Part A: Polym. Chem*., 2009, **47**, 6514.

16 S. Shi, X. Xie, P. Jiang, S. Chen, L. Wang, M. Wang, H. Wang, X. Li, G. Yu, Y. Li, *Macromolecules*, 2013, **46**, 3358.

17 G. Zhao, Y. He, Y. Li, *Adv. Mater*., 2010, **22**, 4355.

18 L. M. Andersson, C. Muller, B. H. Badada, F. Zhang, U. Wurfel, O. Inganas, *J. Appl. Phys*., 2011, **110**, 024509.

19 P. Peumans, A. Yakimov, S. R. Forrest, *J. Appl. Phys*., 2003, **93**, 3693.